

PLASMA LENS WORK AT UCLA

T. Katsouleas, J. J. Su, and J. M. Dawson
University of California at Los Angeles
Department of Physics
Los Angeles, CA 90024 USA

Abstract

The focusing of particles by a thin plasma lens is analyzed with physical, linearized fluid and PIC computational models. For parameters similar to next-generation linear colliders, the plasma lens strength can exceed 100 MG/cm, and the luminosity can be enhanced by an order of magnitude by passing each beam through an appropriate plasma slab. The plasma electrons effect the focusing by shifting so as to (partially or completely) charge neutralize the beam. The effects of spherical aberrations, emittance, plasma boundaries, and non-linear-plasma dynamics on the final spot size are discussed.

I. Introduction

One of the challenges for future e^+e^- high energy linear colliders is to increase the luminosity as the square of the center of mass energy in order to keep the event rate constant. For fixed repetition rate and number of particles this means reducing the spot size of the beams at the interaction point. Recently, plasma techniques capable of extremely strong focusing gradients (order 100 MG/cm compared to 5 kG/cm for typical quadrupole magnet focusing) have been proposed to accomplish such spot size reduction¹⁻⁶.

At least three distinct particle focusing schemes in plasmas have been referred to as plasma lenses, though the physical mechanisms and capabilities of each are quite different. These are (1) focusing of particles by the radial fields of a large-amplitude plasma wave moving with the beam^{6,7}, (2) focusing by the axial magnetic field of a z-pinch plasma carrying a large axial current^{8,9}, and (3) self-focusing due to shielding of a particle beam's space charge by a quiescent plasma^{1-5,10}. It is this latter plasma lens concept that will be examined here.

In this paper we describe simple analytic models to predict limitations on the final spot size produced by a plasma lens including the effects of spherical aberrations and beam emittance (Sec. II). The analytic predictions are then compared to 2-D electromagnetic, relativistic, self-consistent particle-in-cell (PIC) simulations (Sec. III). The results are discussed in Sec. IV with examples given for presently available beam parameters.

II. Analytic ModelsPhysical Description:

To understand the physical mechanism of the self-pinch lens concept, first consider a relativistic electron beam traveling through vacuum. In this case, the repulsive force due to the space charge of all the electrons in the bunch is cancelled (to order γ^2) by the attractive force due to the self-magnetic field of the bunch; thus the beam continues, with essentially constant radius. However, if this same beam now enters a plasma, the plasma electrons respond to the excess charge by shifting away from the beam particles. The remaining plasma ions neutralize the space-charge force within the beam. For positron beams the charge neutralization is equivalent but is due to the plasma electrons shifting in the opposite direction. While the plasma is very effective at shielding the beam's space charge, it is less effective at shielding its current. Thus the beam experiences almost the full effect of its self-generated azimuthal magnetic field. From Ampere's law this is $B_\theta = 2\pi n_b e r$ for a uniform beam density n_b , where $\beta = v/c \approx 1$. This gives a radial Lorentz force

$$F_r \approx 2\pi n_b e^2 r \quad \text{or} \quad (1a)$$

$$F_r/r \approx 2\pi n_b e^2 \approx 3 \times 10^{-9} n_b \text{ gauss/cm} \quad (1b)$$

for n_b in cm^{-3} . For example, a beam similar to that required for a future 5-TeV collider¹¹ might have 4×10^8 particles, $3\text{-}\mu$ radius, and be 100 μ long, so that $n_b \approx 10^{17} \text{ cm}^{-3}$ and $F_r/r \approx 300$ megagauss/cm. This exceeds by four orders of magnitude the equivalent focusing strength of conventional quadrupole magnets. Neglecting limitations due to aberrations, the beam radius at the interaction point (a^*) is inversely proportional to the focusing strength of the final lens (for fixed lens thickness and beam emittance), and the luminosity is proportional to a^{*-2} . Thus the luminosity enhancement from a plasma lens may be considerable.

The simple physical argument given above based on plasma shielding of space charges neglects some important effects such as electron inertia, return currents, and the radial dependence of n_b . All of these are included quantitatively by a plasma wakefield analysis. The physical model is in good quantitative agreement with the wakefield analysis under the following conditions on the beam's scale length and radius:

$$\ell_b \gg c/\omega_p \gg r_b \quad (1c)$$

where c/ω_p is the plasma skin depth ($\sim 5 \times 10^5 n_b^{-1/2}$ [cm], where n_b is the plasma density in cm^{-3}). The first inequality assures that the beam density rises slowly enough that the plasma electrons respond essentially adiabatically to maintain charge neutrality (i.e., without overshooting and oscillating). The second inequality assures that the plasma return current¹² (which follows in a cylinder a few skin depths in radius) flows mainly outside of the beam and so does not reduce the focusing force within the beam.

Wakefield Description:

A formal wakefield analysis of the plasma lens using a cold fluid plasma model has been given previously in Refs. 1 and 2. Here we summarize the results and apply them to determining the aberrations of the lens.

The transverse wakefield is defined as the transverse Lorentz force on a unit charge moving with velocity $\beta = v/c \approx 1$ in the longitudinal (\hat{z}) direction:

$$W_\perp(r, \xi) = (\vec{E} + \vec{\beta} \times \vec{B})_r \approx E_r - B_\theta$$

where the plasma wake is assumed to be a function only of r and $\xi = z - ct$ (e.g., as in the case when the wake is excited by a beam moving at $\vec{v} = c\hat{z}$). The wakefield excited by a relativistic beam of arbitrary density in the (separable) form $n_b = \rho_\perp(\xi)\rho_\perp(r)$ is¹

$$W_\perp = Z(\xi)\partial_r R(r) \quad (2)$$

where

$$Z(\xi) = \pm \frac{4\pi e \rho_b}{k_p^2} \int_{-\infty}^{\xi} d\xi' \rho_\perp(\xi') \cos k_p(\xi - \xi')$$

$$R(r) = \int_0^r r' dr' \rho_\perp(r') I_0(k_p r') K_0(k_p r) + \int_r^\infty r' dr' \rho_\perp(r') I_0(k_p r) K_0(k_p r')$$

where $k_p = 2\pi\omega_p/c$.

Analytic and numerical solutions of these integrals have been obtained previously by several authors^{1-3,13} for various density profiles. Three representative examples — parabolic $\rho_\perp = \rho_0(1-r^2/a^2)$, uniform $\rho_\perp = \rho_0$ for $r \leq a$, and Gaussian $\rho_\perp = \rho_0 e^{-r^2/2a^2}$ profiles — are illustrated in Fig. 1 for $a = .2 c/\omega_p$. One feature of Fig. 1 worth noting is that the deviations from linear focusing (spherical aberrations) are in opposite directions for uniform beam profiles and Gaussian (or parabolic) profiles. This suggests that the aberrations could be significantly reduced if the beam density could be tailored to some intermediate

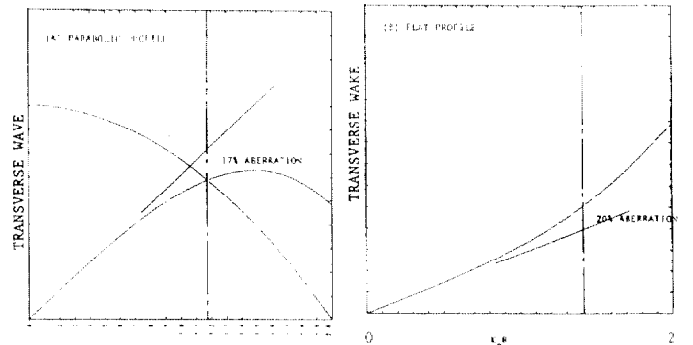


Fig. 1 The focusing force W_\perp vs. r for (a) uniform and (b) parabolic beam density profiles [$\rho_\perp = \rho_0$, $\rho_0(1-r^2/a^2)$, and $a = 2c/\omega_p$].

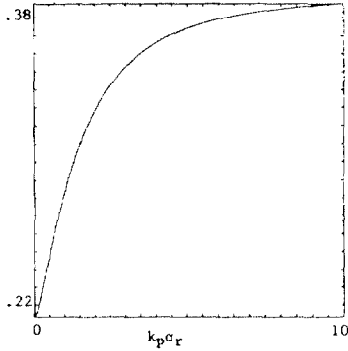


Fig. 2 Spherical aberration ($\equiv 1 - (W_1/r)|_{\sigma} / (W_1/r)|_0$), where σ_r is the r.m.s. radius of the beam) vs. spot size for Gaussian beams.

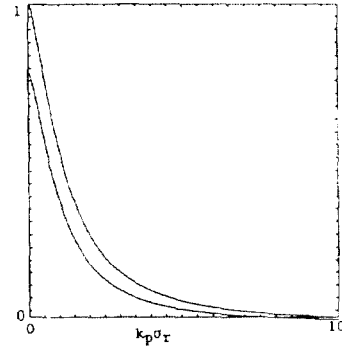


Fig. 3 Focusing strength $W_1/r|_{\sigma}$ vs. spot size for Gaussian beams, normalized to Eq. (1).

profile. The deviation from linear or spherical aberration as a function of spot size (a) is shown in Fig. 2 for Gaussian beams. In Fig. 3 the focusing strength F_r/r vs. spot size (for fixed beam density) is shown. Figure 2 and 3 illustrate the need to keep the spot size small compared to c/ω_p in order to keep the aberrations small and focusing strength large.

Finally, we turn to the z -dependence of the radial wakefield in Eq. (2). As we see from Eq. (2) the solutions to W_1 in general have oscillations in z with period k_p^{-1} . This was missing from our simple physical argument since we neglected the inertia of the electrons. When the plasma electrons are displaced by the particle beam they tend to overshoot and oscillate. A simple solution is to allow the beam density to increase slowly at the head compared to c/ω_p . In this way the plasma electrons respond adiabatically without oscillating appreciably.

A numerical solution of $W_1(z)$ for a slowly rising beam density is shown in Fig. 4. The longer is the scale length of the density rise compared to c/ω_p the smaller are the oscillations in focusing force³ (e.g., for a uniform beam preceded by a linear ramp of length L the ratio of the rippled amplitude to the focusing force is $1/k_p L$). Thus for (narrow) beams ramped up slowly compared to c/ω_p the focusing force is again given by Eq. (1), but with n_0 a function of ξ . The variation in focusing strength over the bunch length gives rise to a "longitudinal aberration" of the plasma lens that will be examined in a future paper.

Spot Size

Two limitations on the final spot size of a particle beam result from the emittance of the beam and the aberrations of the lens. These are illustrated in Fig. 5. Here we use these simple physical pictures and the wakefield results to obtain scaling laws for the final spot size.

The emittance limit on spot size arises because particles entering a lens have angular spread θ_e given by $\theta_e \sim \epsilon/a_0$, where ϵ is the beam emittance (proportional to the transverse phase space area of the beam divided by the beam energy) and a_0 is the spot size at the lens entrance. Thus, two adjacent particles at the lens will spread by an amount $f\theta_e$ by the time they reach the focal point a distance f away. Thus the final spot size will be larger than

$$a^* \geq f\epsilon/a_0 \quad (3)$$

The focal length is easily estimated from the impulse approximation (for a thin lens of thickness $\phi \ll f$) on a particle at radius r .

$$\begin{aligned} \frac{f}{r} &\equiv \frac{P_{||}}{P_{\perp}} = \frac{\gamma mc}{F_r \Delta t} = \frac{\gamma mc}{F_r \phi/c} \quad \text{or} \\ f &= \frac{\gamma mc^2}{F_r \phi} \frac{1}{\phi} \equiv \frac{1}{K\phi} \end{aligned} \quad (4)$$

Combining Eqs. (1), (3), and (4) gives

$$a^* \geq \frac{\epsilon_N}{2} \frac{n_0}{n_b} \left[\frac{1}{K\phi} \right] \left[\frac{1}{k_p a_0} \right] - \frac{\epsilon_N}{\phi a_0} \left[\frac{10^{15} \text{ cm}^{-3}}{n_b} \right] \quad (5)$$

where $\epsilon_N = \gamma\epsilon$ is the normalized emittance in cm-rad and all lengths are in units of cm in the last expression.

The limitation on final spot size due to spherical aberrations is illustrated in Fig. 5(b). A particle at r.m.s. radius a_0 entering the lens is given a radial deflection θ proportional to the focusing strength (K) at radius a_0 . If the lens has aberrations ΔK , then the particle will receive an error in radial kick by an amount $\Delta\theta = \theta(\Delta K/K)$ where $\theta \approx a_0/f$, so that the final spot size is $f\Delta\theta$ or

$$a^* \geq a_0 (\Delta K/K) \quad (6)$$

For the example shown in Fig. 2(a) where $\Delta K/K \sim 17\%$, we would predict a final spot size limit due to spherical aberrations of $a^* \sim .17a_0$.

Thus when both aberrations and emittance are considered, the final spot size will be the larger of Eqs. (5) and (6) (or, when both are comparable, the square root of the sum of the squares⁴).

III. Simulation Model

To verify the simple scaling laws given in Eqs. (1), (5), and (6), we perform 2½D computer simulations of the plasma lens. The simulation code used is ISIS¹⁴; it is a relativistic electromagnetic particle-in-cell simulation code that solves for the self-consistent motion of the plasma and beam particles via Maxwell's equations on a discrete spatial grid. The 2½D spatial and momentum variables are r, z and p_r, p_z , and p_θ .

Figure 6 illustrates real space snapshots of an electron beam passing through a plasma lens. The parameters for this simulation correspond to the analytic/numerical cases in Fig. 1(b) and 4. As expected the low density leading portion of the beam is not well focused, but enables the uniform focusing of the main portion of the beam. The focusing force W_1 within the beam is shown in Fig. 7. These simulation results should be compared to the wakefield model results in Figs. 1(a) and 1(b).

The final spot size of the focused beam is shown in Fig. 8 for four different cases. The first corresponds to a uniform radial density profile and cold beam [as in Figs. 1(a) and (d)]; the last three correspond to a parabolic profile and gradually increasing emittance ($\epsilon = 0, 10^{-3} a_0, 10^{-2} a_0$).

In the first three cases, the spot size is aberration limited. We expect $a^* \sim .2a_0^{m.a.} \sim .3c/\omega_p$ (from Eq. (6) and Fig. 2) for the uniform beam case. The final r.m.s. spot size in the simulation was $\sim 0.1 c/\omega_p$, three times smaller than predicted. The smaller spot size is a reflection of the better than expected linearity of W_1 vs. r (compared Fig. 1(a) and 7(d)). This may be due to a slight change of the beam's density profile within the lens. For the parabolic beam cases, we expect $a^* \sim .2 a_0^{m.a.} \sim .2c/\omega_p$ when the spot size is aberration limited. This is in fair agreement with Figs. 8(b) and (c); though the spot sizes in the simulations are again smaller than predicted (by 30% in these cases). From Eq. (5) we expect the emittance to limit the spot size to a value larger than this when the emittance exceeds $\epsilon \geq .01 a_0$. We see from Figs. 8(c) and (d) that the emittance has little effect when ϵ is one order of magnitude below this ($\epsilon/a_0 = 10^{-3}$), but nearly eliminates the focusing in the last case ($\epsilon/a_0 = 10^{-2}$).

In general, the simulation results corroborate the analytic models. They illustrate transient and boundary effects¹⁴ not included in the analytic models and show that these effects do not substantially alter our conclusions.

IV. Discussion

A number of schemes involving plasmas have the potential to provide ultra-strong focusing of particle beams. The particular plasma lens design that

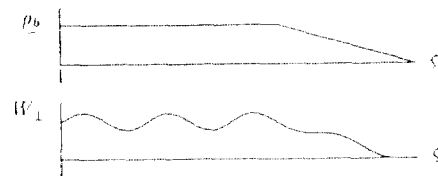


Fig. 4 Solution to Eq. (2) for W_1 vs. z for the linearly ramped beam in the figure showing the slow rise and small oscillations in the focusing force over the length of the beam.

is best depends on the beam's length, width, density and shape. For parameters typical of present e^+e^- colliders we find that the simplest design—a thin plasma slab with no precursors or specialized shaping placed near the final focus of a conventional focusing system—is capable of providing a further enhancement of the luminosity by an order of magnitude.

We illustrate the conclusions of our physical, wakefield and simulation models with a design example for the proposed 1 TeV CLIC collider at the CERN Laboratory in Geneva. The design calls for electron and positron beams of 5×10^9 particles, length $\sigma_z = 200 \mu$, emittance $5 \times 10^{-11} \text{ cm-rad}$ ($\epsilon_N = 10^{-4} \text{ cm-rad}$), and approximately Gaussian profile $n_b \sim n_{b0} \exp(-z^2/2\sigma_z^2 - r^2/2\sigma_r^2)$.¹⁶ The design goal for the final spot size is $a^* = \sigma_r \leq 60 \text{ nm}$.

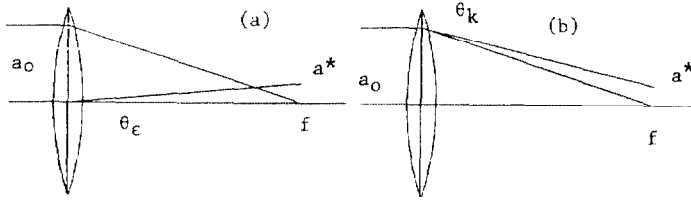


Fig. 5 Illustration of how (a) emittance and (b) spherical aberrations limit final spot size from a lens.

In order to employ a simple self-pinch plasma lens design we must satisfy the following conditions: (1) The initial spot size entering the lens must be small enough to avoid spherical aberration limits. From Eq. (6) and Fig. 2 we expect the aberrations to be on the order of 15%. Thus we take $a_0 = a^*/.15$ or $.4\mu$. (2) The beam should be both long and narrow compared to c/ω_p (inequalities [1c] and [1d]). This specifies a range of plasma densities between $6 \times 10^{14} \text{ cm}^{-3}$ and $1.6 \times 10^{20} \text{ cm}^{-3}$. (3) The initial beam density should be small compared to the plasma density. For the above parameters $n_{b0} \sim 1.4 \times 10^{18} \text{ cm}^{-3}$, so we take $n_0 = 10^{19} \text{ cm}^{-3}$ to satisfy the latter two conditions. (4) The thickness of the lens (ϕ) must be chosen large enough to overcome the emittance of the beam (inequality [5]) and small enough compared to f [Eq. (4)] to justify our use of a thin lens treatment. These give $\phi \geq 1.8 \text{ mm}$ and $f \sim 4.6 \text{ cm}$. Thus a thin plasma slab of thickness 2 mm and density 10^{19} cm^{-3} placed 4 cm from the interaction point should be capable of reducing the radius of the e^+ or e^- beams from $\sim .4\mu$ to $\sim 60 \text{ nm}$.

Although the linear lens design just described applies to both electrons and positrons, it may be advantageous to employ a non-linear-plasma lens design ($n_b > n_0$) for the electrons. The non-linear design not only has smaller aberrations ($<3\%$ in simulations we have performed) but also a lower density, so the contribution to background noise in the detectors from collisions in the plasma will be less.¹⁷

If suitable means of producing high-repetition-rate plasmas (such as laser-ionized laminar gas jets¹⁸) prove feasible, then plasma lenses may become a promising means of attaining unprecedented spot sizes.

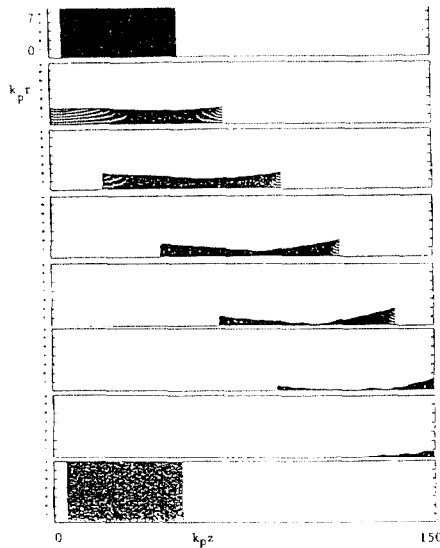


Fig. 6 Real space (r vs. z) for a beam and a plasma at several times showing focusing in a 2-D PIC simulation. The beam density was linearly ramped over $30 c/\omega_p$ in z and constant for $40 c/\omega_p$ with a peak density of $.2n_{p0}$, energy $\gamma = 200$. The radial profile was parabolic out to radius $a = 2 c/\omega_p$. The lens is a thin plasma slab of thickness $50 c/\omega_p$.

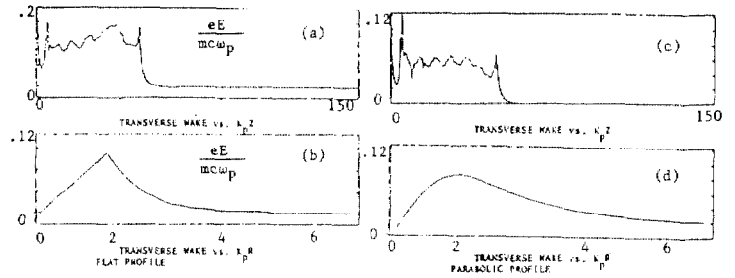


Fig. 7 The focusing force W_1 in the simulation of Fig. 6 as a function of (a) z at $r = 1.7 c/\omega_p$ and (b) r at $z = 35 c/\omega_p$. In (c) and (d) the corresponding results of a simulation with a uniform radial beam profile (out to radius $2c/\omega_p$) are shown.

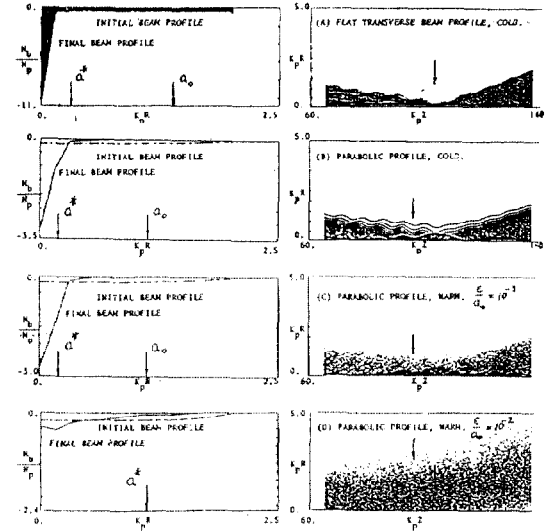


Fig. 8 Beam densities vs. r (left) and real space of beam (right) at the final focus in various 2-D plasma lens simulations: (a) flat, cold beam; (b) parabolic, cold beam; (c) parabolic, warm beam ($\epsilon = 10^{-3} a_0$); (d) parabolic, warmer ($\epsilon = 10^{-2} a_0$). All other parameters are as in Fig. 7.

References

1. P. Chen, Particle Accelerators **20**, 171 (1987).
2. P. Chen, J. J. Su, T. Katsouleas, S. Wilks and J. M. Dawson, IEEE Trans. Nucl. Sci. PS-15, 218 (1987).
3. J. B. Rosenzweig, B. Cole, D. J. Larson, D. B. Cline, WISC-EX-85-0000, submitted to Particle Accelerators (1987).
4. D. B. Cline, B. Cole, J. B. Rosenzweig, J. Norem, Proc. IEEE Particle Accelerator Conference, 241 (1987).
5. J. B. Rosenzweig and P. Chen, SLAC-PUB-4571, March 1988.
6. P. J. Channell in Laser Acceleration of Particles (Malibu, 1985) AIP Conference Proceedings No. 130, C. Joshi and T. Katsouleas, eds. (AIP, NY, 1985); J. D. Lawson et al., Rutherford-Appleton Laboratory Report No. RL 83057, 1983 (unpublished).
7. R. Fedele, U. de Angelis, T. Katsouleas, Phys. Rev. A **33**, 4412 (1986).
8. B. Autin et al., IEEE Trans. Plasma Sci. PS-15, 226 (1987).
9. T. G. Roberts and W. H. Bennett, Plasma Physics **10**, 381 (1968).
10. T. Katsouleas, Phys. Rev. A **33**, 2056 (1986).
11. B. Richter in Laser Acceleration of Particles (Malibu, 1985) AIP Conf. Proc. No. 130, C. Joshi and T. Katsouleas, eds. (AIP, NY, 1985).
12. J. L. Cox, W. H. Bennett, Phys. Fluids **13**, 182 (1970); R. Keinigs and M. E. Jones, Phys. Fluids **30**, 252 (1987).
13. J. J. Su et al., IEEE Trans. Plasma Sci. PS-15, 192 (1987).
14. G. Gister, M. Jones, C. Snell, Proc. 11th Int'l Conf. Num. Sim. of Plasma, (Quebec, Canada, 1985), paper 1-B-01.
15. Mtingwa, submitted to Phys. Rev. A (1987); in this Ref., transient effects on the longitudinal wakefield at a plasma boundary are addressed.
16. E. J. N. Wilson, private communication.
17. The effect of scattering in the plasma on beam focusing was shown to be negligible by R. G. Evans, Proc. ECFA Workshop on New Developments in Part. Accel. Techniques (Orsay, France, 1987); however, the concern here is over event noise reaching the detectors.
18. A. E. Dangor et al., IEEE Trans. Plasma Sci. PS-15, 161 (1987); J. Norem, Argonne National Lab Report No. ANL-HEP-TR-87-77 (Sept., 1987), unpublished.